Elasto-Kinematic Calibration of the Lunar Rover Mini 6 DOF Robotic Arm

Conenna, Marco; Guo, Jian; Wedler, Armin

DOI
10.1007/978-3-031-89471-8_25

Publication date
2025

Document Version
Final published version

Published in
European Robotics Forum 2025 - Boosting the Synergies between Robotics and AI for a Stronger Europe

Citation (APA)
Conenna, M., Guo, J., & Wedler, A. (2025). Elasto-Kinematic Calibration of the Lunar Rover Mini 6 DOF Robotic Arm. In M. Huber, A. Verl, & W. Kraus (Eds.), *European Robotics Forum 2025 - Boosting the Synergies between Robotics and AI for a Stronger Europe* (pp. 162-167). (Springer Proceedings in Advanced Robotics; Vol. 36 SPAR). Springer Nature. https://doi.org/10.1007/978-3-031-89471-8_25

Elasto-Kinematic Calibration of the Lunar Rover Mini 6 DOF Robotic Arm

Marco Conenna[1(✉)], Jian Guo[1], and Armin Wedler[2]

[1] Faculty of Aerospace Engineering, Delft University of Technology, 2629HS Delft, The Netherlands,
marco.conenna01@gmail.com, j.guo@tudelft.nl
[2] Deutsches Zentrum für Luft- und Raumfahrt e.V., Wessling, Germany,
armin.wedler@dlr.de

Abstract. Inaccuracies in robotic arms can significantly hinder their performance in tasks where precision is critical. This paper focuses on the kinematic calibration and elasticity compensation of the six degrees of freedom robotic arm integrated into the Lunar Rover Mini, developed in collaboration with the Robotics and Mechatronics Institute of the German Aerospace Center (DLR), Wessling. The arm, constructed using 3D-printed components and driven by affordable RC servo motors, experiences notable inaccuracies in end-effector positioning due to joint flexibility and structural deformation, especially under load. This research aims to enhance the arm's accuracy through a model-based calibration approach that compensates for both elastic deformations and geometric misalignments, addressing the absence of feedback sensors. This cost-effective approach, which requires only 3D measurements of the end-effector's position, has resulted in an approximately 80% reduction in the robotic arm's average position error, proving advanced robotic technologies can be more accessible for educational and research applications.

Keywords: Robotic Arm, Elastic Calibration, Precise Manipulation, Cost-Effective Robotics, End-Effector Accuracy, 3D-Printed.

1 Introduction

1.1 Motivation

The Lunar Rover Mini (LRM) [1] developed within the Robotics and Mechatronics Institute of DLR, is a 6-wheeled terrestrial designed to serve as a cost-effective learning platform which students and researchers can exploit to research multiple areas of robotics. At the end of 2023, LRM was equipped with a six degrees of freedom (DOF) robotic arm, exponentially broadening its educational applications and aligning it closer to the more sophisticated systems developed in the institute.
The robotic arm of LRM has been designed to meet the rover's objectives, aiming to provide a cost-effective yet capable alternative to existing systems in the market.

To achieve this goal, the motors used in the joints are commercially available radio-controlled (RC) servos, and the entire structure is 3D printed in acrylonitrile styrene acrylate (ASA), except for steel inserts used to connect the servo heads to the links.
Preliminary tests conducted during a testing campaign in the analogue environment of Vulcano, Italy (1), revealed that the high torque experienced by the small motors caused deflection in the joints, significantly hindering the accuracy of the end effector's position. While the design meets the cost requirements, it falls short of the performance expectations, rendering the arm inadequate for its intended purpose of high-level research.

Fig. 1. The Lunar Rover Mini during the testing campaign in Vulcano, Italy.

1.2 Problem Statement

This work addresses the inaccuracies in the position of the LRM arm's end effector caused by the elasticity of its joints and links observed during preliminary tests. The significant challenge of the lack of feedback sensors in the motor joints, driven by RC servos, necessitates a model-based compensation approach. This leads to the following research question:
How can a 6 DOF 3D-printed robotic arm, constructed with low-cost motors, improve its accuracy through model-based joint deflection compensation?

2 Related Work

According to Karan and Vukobratovic in [4], the primary sources of inaccuracies in such systems fall into six categories: environmental (e.g., temperature changes), parametric (variation of kinematic parameters, joint offsets), measurement (sensor resolution and nonlinearity), computational (round-off errors), and application errors (installation and workpiece position errors). Some factors can only be prevented, while others require mitigation and correction afterwards. Environmental factors fall into the first category and can be addressed by selecting materials carefully during the design phase. In contrast, assembly, manufacturing, and elasticity factors are reduced in design and further corrected through calibration.
The state of the art provides a solid foundation for the calibration methodology required. As introduced in Section 1.2, the LRM's arm requires model-based calibration to address joint elasticity, needing three fundamental steps [2]. First is sensor calibration to correct inaccuracies in sensor readings, ensuring the actual angle of the joint aligns with the commanded angle. Second, an accurate geometric calibration to address deviations in the robot's kinematic structure.

Third and most relevant to our work is elastic calibration, which accounts for the structural flexibility and joint compliance within the system. While this level is crucial, the earlier levels are necessary, as each calibration layer builds upon the previous one. For this reason, the most complex level takes the name of "Elasto-Kinematic Calibration".
Kamali et al. in [3] define four steps for this advanced calibration. First, a kinematic model of the arm is developed using the Product of Exponentials (POE) or Denavit-Hartenberg (DH) convention. This model should also incorporate a parametrization of the errors affecting the end-effector's position, represented by the vector $\boldsymbol{\nu}$. The kinematic model will have the shape of $\boldsymbol{x} = f(\boldsymbol{\theta}, \boldsymbol{\nu})$ with $\boldsymbol{\theta}$ the [6×1] configuration vector with the angles of each joint. Secondly, an external measurement device must capture the end-effector's position across various poses. The group of poses $\boldsymbol{\Psi}$ that must be measured is the one that maximises the Observability Index, defined by Joubair et al. in [5] as:

$$O = \frac{\sqrt[m]{\sigma_1 \sigma_2 \cdots \sigma_m}}{\sqrt{(n)}} \tag{1}$$

where n is the number of calibration measurements, m is the number of parameters in $\boldsymbol{\nu}$, and $\sigma_{1...m}$ are the singular values of the Jacobian Identification Matrix's SVD (Singular Values Decomposition). This matrix represents the relationship between the pose errors in the calibration configurations and the parameters. It's a [3n×m], and each [3×m] row is calculated as:

$$\boldsymbol{J}^k(\boldsymbol{\nu}, \boldsymbol{\theta}) = \frac{\partial f(\boldsymbol{\theta}^k, \boldsymbol{\nu})}{\partial \boldsymbol{\nu}} \tag{2}$$

An important aspect of the numerical computation of $\boldsymbol{J}$ is the necessity of selecting an appropriate step size to prevent numerical instability.
The third step involves comparing these measured positions with those predicted by the forward kinematics and using regression to identify the parameter vector $\boldsymbol{\nu}$. Finally, the forward kinematics are corrected using the identified $\boldsymbol{\nu}$.

3 Elasto-Kinematic Calibration

Following the three calibration levels approach, the methodology described in Section 2 has been applied to LRM. The 1st level calibration will match the RC servos PWM signal to the angle of each joint, while the 2nd and 3rd will correct via a parameter-based strategy the kinematic offsets and elastic deformations.

3.1 1st Level Calibration: PWM Signal Tuning

RC servos are commanded through a Pulse Width Modulation (PWM) signal, which the manufacturer specifies between 900 and 2400 μs, nominally corresponding to ±100°. However, due to the manufacturing process and the inaccuracy in the positioning of the servo motor encoder, these values must be calibrated. To tackle this issue, a device similar to a protractor was designed to

measure angles at three key points: -100°, 0°, and +100°, and find the relative PWM frequencies. In the arm's control software, two linear interpolations were then applied, one between -100° and 0° and another from 0° to +100°.

3.2 Model

Given its simplicity and the extensive literature, the DH convention was chosen for the kinematic model. For a 6 DOF arm, this involves defining the kinematic parameters θ, α, d, and a. With the kinematic model established, the set of error parameters that make up $\boldsymbol{\nu}$ is formed by adding an uncertainty δ to each parameter. Additionally, three translational parameters (x, y, z) and three rotational parameters ($\alpha,\ \beta,\ \gamma$) are added for both the base of the arm and the end-effector relative to the preceding link. Next, joint elasticity is modelled by assuming linear elasticity and introducing the elastic parameter k, so that the configuration angles are expressed as $\theta_i + \delta\theta_i + k_i\tau_i$, where τ_i represents the torque acting on joint i. Preliminary tests revealed bending in the 3D-printed base, leading to an additional elastic parameter for the base rotation angle β, defined as $\beta + \delta\beta + k_0\tau_0$, and expanding $\boldsymbol{\nu}$ to 43 elements.
To ensure success in the subsequent identification phase, the model must be simplified by considering only the linearly independent parameters. This can be achieved by examining the rank of the Jacobian Identification Matrix $\boldsymbol{J}$ (2) and systematically eliminating parameters until it aligns with the length of $\boldsymbol{\nu}$. Through this process, the number of parameters is reduced to 28.
To finalize the elasto-kinematic model, it was essential to weigh the mass of each link and identify its centre of mass. In this case, a turning machine was employed to securely hold each piece between two points, adjusting the contact points until the part could spin freely. Once the centre of mass was integrated into the forward kinematics, the elasticity was corrected by adjusting iteratively each joint's deflection based on the torque acting on it.
Three modelling options were considered: 1) Elasto-Kinematic (28 parameters); 2) Purely Kinematic (21 parameters); 3) Purely Elastic (7 parameters).

3.3 Measurements

The ART (Advanced Realtime Tracking) system was used to measure the 3D position of the end-effector in different poses. This required the design of two 3D-printed targets using IR reflective spheres, one for the end-effector and the other for the base structure to be used as a reference. The end-effector target was designed to accommodate weights, enabling two sets of measurements: one under no load and another with a 66.3 g load applied at the end-effector. This sampling allowed a deeper analysis of the system's behaviour during the two operational phases: approaching and retrieving the target.
Before conducting the 6 DOF arm measurements, the servo of one joint was tested individually to establish a baseline elastic coefficient k, which was later used as a reference in the identification phase. The result is a nearly elastic behaviour, with coefficients ranging between $2.36 \cdot 10^{-2}$ and $3.42 \cdot 10^{-2}$ rad/Nm.

Benefiting from the PWM tuning, the arm configurations for measurement included each joint positioned at -100°, 0°, and 100°, totalling $3^6 = 729$ possible poses. A collision avoidance algorithm was implemented to prevent potential self-collisions or contact with the surrounding environment, reducing the number of safe and measurable poses to 393.

3.4 Parameters Identification

The last step is identifying the parameters for each option and integrating them into the forward kinematics. The methodology consists of applying a least squares method, which adjusts the parameter values to part of the measured data, while the rest will be used in the validation phase. Only 50 poses are used for the identification, and they are determined based on the group $\boldsymbol{\Psi}$ that maximises the observability index (1). $\boldsymbol{\Psi}$ is specific to each option and is found employing the DETMAX sorting algorithm [6], which was then updated with physical constraints to prevent negative values for the joints' elasticity.
The identification was conducted on both measurement sets: one with the end-effector unloaded and the other with a 66.3 g load applied. This approach facilitates the assessment of the model's accuracy under varying loads applied to the end-effector.

4 Results & Conclusions

The results of the identification process show elastic coefficient values ranging from $8.06 \cdot 10^{-3}$ to $2.17 \cdot 10^{-1}$ rad/Nm in the elasto-kinematic case (Option 1), and from $2.29 \cdot 10^{-2}$ to $5.08 \cdot 10^{-1}$ rad/Nm in the purely elastic case (Option 3). As expected, the purely elastic case presents higher values, as the elasto-kinematic approach partially compensates for inaccuracies through kinematic offsets. Moreover, the $\sim 3 \cdot 10^{-2}$ rad/Nm measured during the preliminary tests falls in the identified range.
Figure 2 shows a comparison of the 3D position errors of the end-effector when integrating the different sets of $\boldsymbol{\nu}$, one for each modelling option, into the forward kinematics of the arm. The configurations used for this comparison are the portion of the 393 measured poses with a 66.3 g load at the end-effector, not included in the identification phase, thus not part of $\boldsymbol{\Psi}$.
As expected, the elasto-kinematic calibration is the best-performing parametrization, reducing the 3D end-effector position error norm of 82.8%, from an average of 32.9 mm to 5.65 mm. A notable insight is that elastic calibration improves the arm's accuracy by 70%, compared to 42% with purely kinematic calibration, reducing average errors to 10 mm and 19 mm, respectively. This outcome confirms that elasticity has a more significant influence than kinematic offsets, as anticipated.
As a final step, $\boldsymbol{\nu}$, identified using measurements with a 66.3 g load at the end-effector, was tested on measurements taken with no load and vice versa, demonstrating functionality in both cases with accuracy improvements ranging

from 81% to 83%.
In conclusion, the methodology proved successful, enhancing the arm's mean accuracy by approximately 80% and demonstrating that only 50 specific 3D end-effector position measurements will be required for future recalibrations.

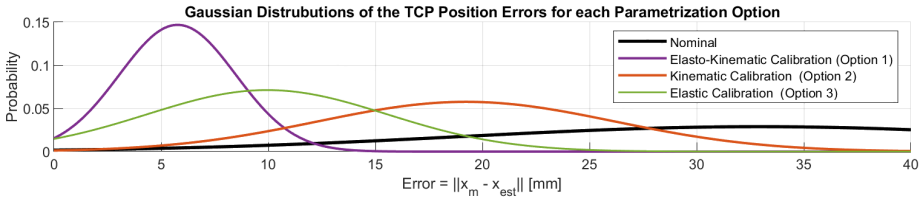

Fig. 2. Plot of the norm of the 3D position error distribution for each option when applying the corrected forward kinematics on the 343 poses not chosen for the identification phase, with a load of 66.3 g at the end-effector.

5 Acknowledgements

We especially thank DLR and TU Delft for supporting this project. A special acknowledgement also goes to the Helmholtz Association for funding the testing campaign through the iFOODis project (contract no. KA-HSC-06 iFOODis).

References

1. Bekkers, S., Bettendorf, M. T., Reill, J., Giubilato, R., & Wedler, A. (2023, October). The Lunar Rover Mini: Towards a versatile, open-source mobile robotic platform for educational and experimental purposes. 17th Symposium on Advanced Space Technologies in Robotics and Automation. https://elib.dlr.de/202313/
2. Elatta, A. Y., Gen, L. P., Zhi, F. L., Daoyuan, Y., & Fei, L. (2003). An Overview of Robot Calibration. Information Technology Journal, 3(1), 74–78. doi:10.3923/itj.2004.74.78
3. Kamali, K., Joubair, A., Bonev, I. A., & Bigras, P. (2016, May). Elasto-geometrical calibration of an industrial robot under multidirectional external loads using a laser tracker. 2016 IEEE International Conference on Robotics and Automation (ICRA). doi:10.1109/icra.2016.7487630
4. Karan, B., & Vukobratović, M. (1994). Calibration and accuracy of manipulation robot models—An overview. Mechanism and Machine Theory, 29(3), 479–500. doi:10.1016/0094-114x(94)90130-9
5. Joubair, A., & Bonev, I. A. (2013). Comparison of the efficiency of five observability indices for robot calibration. Mechanism and Machine Theory, 70, 254–265. doi:10.1016/j.mechmachtheory.2013.07.015
6. Mitchell, T. J. (1974). An algorithm for the construction of 'D-optimal' experimental designs. Technometrics: A Journal of Statistics for the Physical, Chemical, and Engineering Sciences, 16(2), 203. doi:10.2307/1267940